Int. J Multiphase Flow Vol 12, No 4, pp 531–541, 1986
Printed in Great Britain

0301-9322/86 $3.00 + .00
Pergamon Journals/Elsevier

FLOODING IN AN ELBOW BETWEEN A VERTICAL AND A HORIZONTAL OR NEAR-HORIZONTAL PIPE

PART I: EXPERIMENTS

H. SIDDIQUI and S. BANERJEE
Department of Chemical and Nuclear Engineering, University of California, Santa Barbara, CA 93106, U.S.A.

and

K. H. ARDRON
Thermalhydraulics Research Branch, Whiteshell Nuclear Research Establishment, Atomic Energy of Canada Limited, Pinawa, Manitoba ROE 1LO, Canada

(*Received* 6 *September* 1984, *in revised form* 20 *October* 1985)

Abstract—Measurements are described of flooding limits in countercurrent air-water flow through pipe elbows consisting of an upper vertical leg and a lower leg which is horizontal or slightly inclined. Results indicate that flooding is caused by unstable wave formation (slugging) at the hydraulic jump which forms in the lower pipe limb close to the bend. The gas flow velocities at flooding are well below those expected for vertical pipes, and are found to depend on tube diameter, the length of the lower limb, and on the radius of curvature of the bend. A correlation is given between the nondimensional gas velocity and the void fraction at the location of the hydraulic jump at the inception of flooding.

1. INTRODUCTION

In countercurrent gas–liquid flow in a tube, a limit is reached when the liquid downflow cannot be increased any further by increasing liquid supply to the top of the tube. This limit is called "flooding".

Flooding in vertical tubes and annuli has been studied extensively because of its importance to the chemical industry and in some postulated loss-of-coolant accidents (LOCAs) in nuclear reactors. Empirical correlations due to Wallis (1969) and Pushkina & Sorokin (1969) are commonly used to predict vertical flow flooding. We will not review the literature on correlations here because a recent report by Tien *et al.* (1979) contains such information. Several theoretical models of vertical flow flooding have been developed based on consideration of the motion of unstable interfacial waves (e.g., Shearer & Davidson 1965; Richter 1981), although none of these has yet found general acceptance.

The problem of flooding in horizontal tubes has received little attention compared with the vertical case. Some of the first experiments reported were conducted by Wallis & Dobson (1973) who studied countercurrent air–water stratified flow in a rectangular duct. They found that as the air flow rate was increased, a critical condition was reached at which rapid wave growth (slugging) occurred. Beyond this point the liquid flow could no longer be sustained at its previous value, indicating the onset of flooding. Richter *et al.* (1978) and Krowlewski (1980) measured flooding limits in air–water countercurrent flows in horizontal tubes connected at the inlet to either 45° or 90° elbows where the elbows lie in the vertical plane. These experiments show that the gas flow rate required to produce flooding in an elbow geometry is much smaller than would be needed for a vertical tube. Flooding in elbows is of importance in several applications. For example, in a light-water reactor the elbows between the pressurizer and the hot-leg affect the rate at which the pressurizer can drain, in certain small break LOCAs. In the CANDU pressurized heavy water reactor, flooding in the elbows in the feeder pipes may affect the rate at which emergency cooling water is delivered to the reactor core in some postulated large break LOCAs.

The previous experiments on flooding in the vicinity of elbows were conducted over a limited range of conditions, so that effects of important parameters, such as tube diameter,

length and inclination of the lower limb, and radius of curvature of the elbow, were not clear. To develop predictive capability for the onset of flooding in such geometries, it was felt that more extensive experiments were needed.

To this end, atmospheric pressure air–water experiments were carried out with the following range of parameters in a vertical-to-horizontal (liquid flow direction) 90° elbow:

(i) 36.5 mm $\leqslant$ pipe diameter $\leqslant$ 47 mm;
(ii) 24 $\leqslant$ horizontal leg length to diameter ratio $\leqslant$ 95;
(iii) square edge $\leqslant$ elbow radius of curvature $\leqslant$ 300 mm.

Limited experiments were also carried out with elbows in which the lower limb was slightly inclined with respect to the horizontal.

The results of these experiments are discussed in this paper, and correlations are proposed for the onset of complete liquid carry-up, and for the onset of flooding based on "local conditions" in the lower limb of the elbow near the bend. In the second paper in this series (part II), a two-fluid model is used to calculate the local conditions, and a more general flooding correlation incorporating the effect of the length and inclination of the lower limb of the elbow is developed.

2 EXPERIMENTAL ASPECTS

A schematic of the experimental rig is shown in figure 1. The main components of the system are the test section, the air supply, the liquid recirculation system, and the instrumentation.

Air was fed, after metering, to the test section from a vertical cylinder that leveled out pressure oscillations in the supply line and also acted as a separator. The pressure in the cylinder was monitored and controlled manually. The water in the system was stored in a stainless steel surge tank and recirculated to the sintered part of the vertical leg of the test section. The large pressure drop across the sintered part of the test section ensured a constant-flow inlet condition. The test sections were made from acrylic plastic or glass, and allowed flow visualization.

Flooding conditions were initiated by gradually increasing the air flow rate, for a fixed water flow rate, until flooding was visually observed. The pressure drop across the elbow was also measured to confirm the visual measurements. A rapidly fluctuating ΔP signal indicated the onset of flooding.

In flooding conditions, a portion of the water was carried upward and was collected in a graduated overhead tank made of glass (see figure 1). The carry-over rate was determined from the level rise in the tank. A deflector separated the water flow from the air stream.

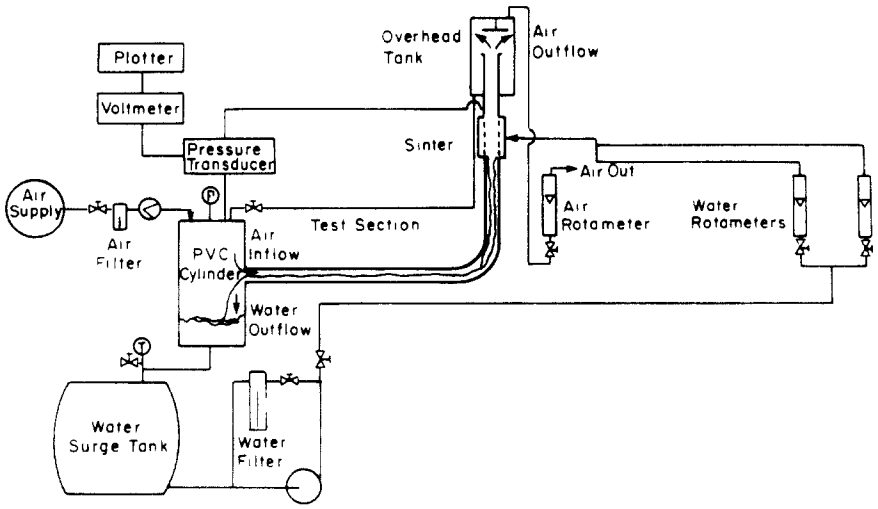

Figure 1 Schematic diagram of the experimental rig

The air was vented at the top of the glass tank through a rotameter. The water flowed back to the water storage tank after separation. Apart from obtaining the data for the onset of flooding, the conditions leading to total carry-up (or zero liquid penetration) were also determined.

In the majority of tests the lower limb of the elbow was horizontal. The inclination was checked periodically by inspecting the slope of a layer of still water in the tube. Slight variations in the inclination occurred between these inspections which were corrected. By this means the angle of inclination with respect to the horizontal was maintained within the limits $\pm$ 0.03°.

Tests with the vertical-to-horizontal elbow configuration were conducted with tubes of 36.5, 38, 44, and 47 mm diameter, and bend radii of curvature O (square), 60, 90, 150, 225, and 300 mm. For each tube diameter an individual sinter piece was made to precisely fit the test section. A schematic design of the sinter which served to introduce water into the test section is shown in figure 2.

The elbows were made in our laboratory by bending lengths of straight tubing. While great care was taken to keep the pipe cross section circular, the cross sections were always slightly elliptical in the bend region.

Several supplementary experiments were conducted to investigate the effect of varying the inclination of the lower limb of the elbow, the effect of flow geometry at the air inlet end of the test section, and the effect of placing a weir at the water outlet. High-speed motion pictures of the flooding and carry-up phenomena in the transparent test section were also taken.

3. RESULTS AND DISCUSSION

In the following, the experimental results described are for cases where the lower limb of the elbow was horizontal, unless it is stated otherwise.

3.1 Visual observations

Flooding, as observed in our experiments, appears to result from an interfacial instability arising from interaction between the gas and the liquid streams.

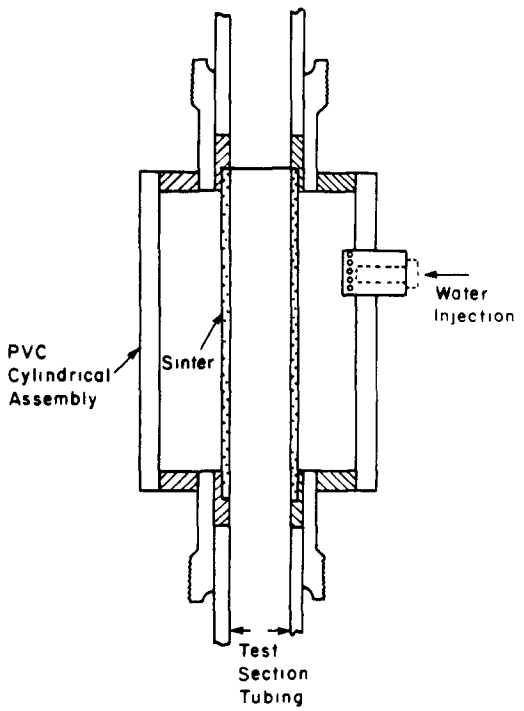

Figure 2. Schematic diagram of sinter assembly

Consider first the water flowing down the vertical section and around the bend as shown in figure 1. A hydraulic jump in water level was usually observed in the horizontal leg near the bend. The location of the hydraulic jump depended on the water flow rate. At higher water flow rates, the hydraulic jump moved away from the bend. For very low water flow rates (less than 315 g/s for the range of tube diameters studied) the hydraulic jump was very weak and difficult to observe.

The reasons for the formation of the jump are clear. The water flows down the vertical section as a thin liquid film of high velocity. As it comes around the bend, this liquid velocity exceeds the gravity wave velocity (i.e. the Froude number is well above unity), leading to a hydraulic jump. The liquid is introduced axisymmetrically in the vertical section, and while the distribution may change somewhat due to the air flow coming up from the bend being skewed, the pattern remains largely axisymmetric compared to the horizontal section. The liquid flows at the bottom of the tube in the horizontal section; this means that liquid drains from the top of the tube to the bottom in the bend region, giving rise to a complex flow pattern which makes prediction of the jump height difficult.

In carrying out the experiments it was noticed that the water depth not only depended on the flow rates but also varied along the channel—there was a gradual decrease in water height from the location of the hydraulic jump towards the water outlet. Therefore frictional losses in the horizontal run cannot be ignored in describing the flooding process. At low air flow rates, the water surface was quite smooth and glassy. At higher air flow rates, wind-generated, near-sinusoidal waves appeared on the interface, moving in the direction of air flow. The amplitude of these waves varied with time, and along the length of the tube With increasing air flow rates, the hydraulic jump was dragged towards the bend, and eventually a point was reached at which a slight increase in air flow rate initiated slugging. High speed movies indicated that an instability occurred at the crest of the hydraulic jump, causing bridging of the pipe. Once bridging was initiated at the hydraulic jump, water started to load the vertical section of the tube and was eventually carried above the water injection point. Thus, the inception of flooding could be identified with the occurrence of slugging at the hydraulic jump in our experiments.

3.2 Flooding limits

A general picture of how the data compare with correlations for vertical and horizontal tubes is presented first, followed by a discussion of the parametric effects Experimental data presented in terms of the usual nondimensional parameters j_G^* and j_L^* are shown in figure 3 The j^* parameters are defined by $j_k^* = j_k/\sqrt{gD(\rho_L - \rho_G)/\rho_k}$, where j_k and ρ_k

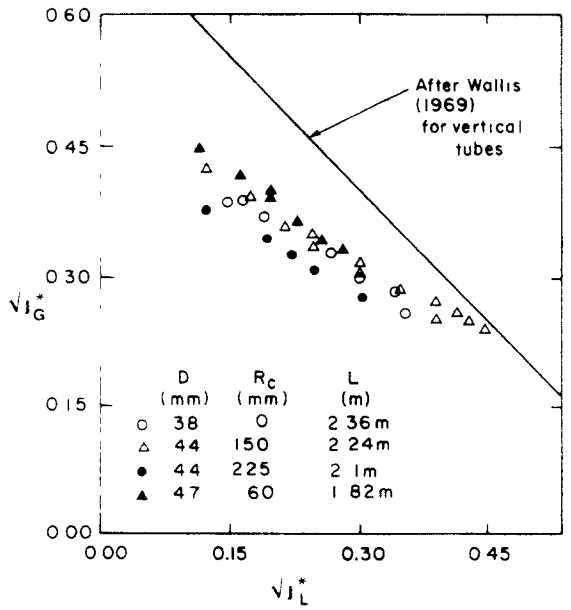

Figure 3 Flooding limits for several vertical–horizontal elbows

are the superficial velocities and densities of phase k ($k = G$ for the gas phase and $k = L$ for the liquid phase), D is the tube diameter, and g the gravitational acceleration. Also shown in figure 3 is a commonly used form of Wallis (1969) correlation for flooding in a vertical tube which has the equation $j_G^{*1/2} + j_L^{*1/2} = 0.7$. (Figure 3 is given for illustrative purposes only to give a comparison with flooding behavior in vertical tubes. It should be recognized at the outset that the onset of countercurrent flow breakdown (flooding) in a system of the type considered here will depend on the length of the horizontal section, and therefore the $\sqrt{j_G^{*1/2}}$ vs. $\sqrt{j_L^{*1/2}}$ parameters would not be expected to define the flooding curves uniquely.) It can be seen that in general the onset of flooding in bends takes place at lower air flow rates than in vertical tubes, for the same water flow rates. This is not surprising since the wave instability causing flooding occurs in the horizontal section.

Figure 4 shows experimental results, using the coordinate system F and X proposed by Taitel & Dukler (1976) to describe the transition between stratified and slug flow in horizontal cocurrent flow. Here F is a Froude number for the gas phase, which is identical to the parameter j_G^* defined above; X is the Martinelli parameter, defined by $X^2 = |(dp/dx)_L|/|(dp/dx)_G|$, where $(dp/dx)_k$ refers to the frictional pressure drop if one phase alone flowed in the horizontal section of the pipe. D, L, and R_c referred to in the figure denote the internal diameter and length of the horizontal pipe, and the radius of curvature of the bend. The curve in figure 4 is a prediction of the Taitel–Dukler model for the transition to slugging in cocurrent flow. It is seen that the present data for flooding in bends in countercurrent flow lie considerably below the slugging transition line expected in cocurrent flow.

It is clear that correlations for flooding in vertical tubes, or for transitions to slug flow in horizontal tubes, do not predict the present data satisfactorily.

We now examine the effects of the various geometrical parameters on the experimental results.

Horizontal length effect. Experiments were performed in which the length-to-diameter ratio (L/D) of the horizontal leg was varied. Results are displayed in figure 5 in terms of the j^* parameters defined above. It is clear that a longer horizontal length leads to lower velocities for onset of flooding. This is to be expected, as longer horizontal lengths cause the liquid level to be higher in the vicinity of the bend, leading to a higher gas velocity and hence an earlier onset of unstable wave growth at the hydraulic jump.

The effective length of the horizontal section can also be varied by inserting a weir at the water outlet. Two weir heights were investigated in the present work and the results

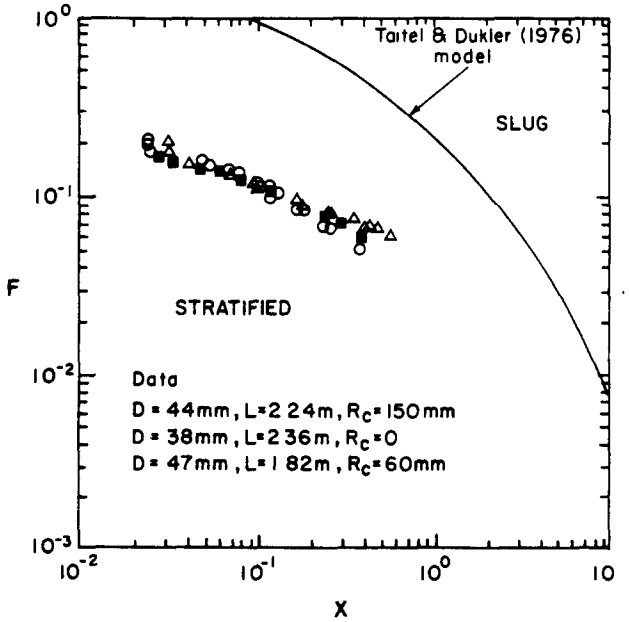

Figure 4. Flooding limits for several vertical–horizontal elbows.

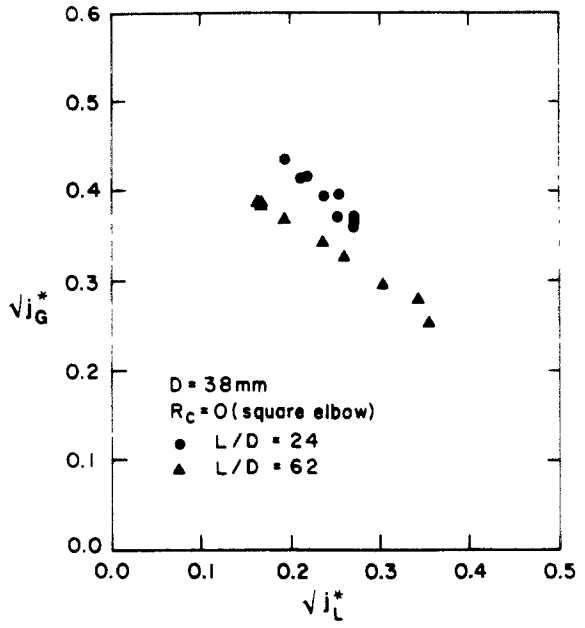

Figure 5 Effect of horizontal length on flooding (square elbow)

are shown in figure 6. Flooding occurs at considerably lower flow rates when the weir height is increased from 12.7 to 16 mm in a 44 mm I.D. pipe. The conclusion from these results is that the length of the lower leg must be taken into account when predicting flooding data in these flow geometries. A quantitative evaluation of the length effect is given in part II.

Bend radius of curvature. Another important parameter was found to be the bend radius of curvature R_c. Data are shown in figure 7. It is seen that larger radii lead to onset of flooding at lower gas flow rates. This effect is particularly noticeable after $\sqrt{j_L^{*1/2}}$ exceeds about 0.25.

The reasons for the changes in flooding conditions caused by a change in bend radius are not fully understood. The effect probably occurs because of the change in the shape of

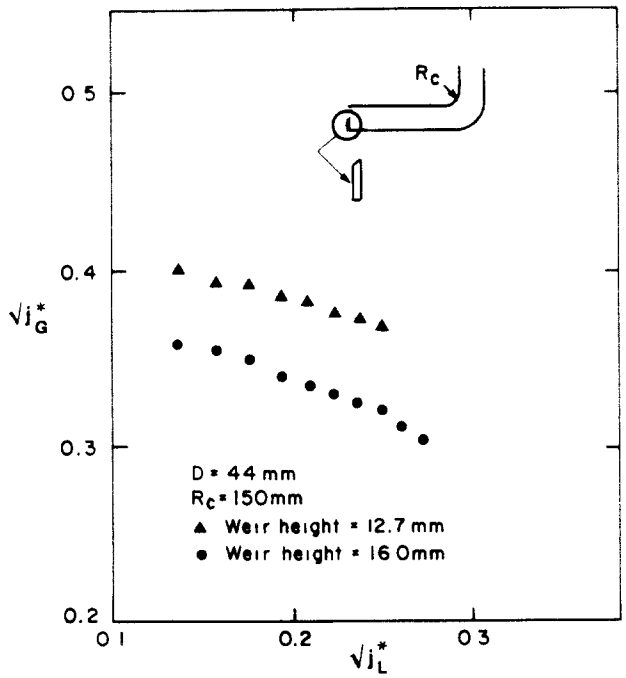

Figure 6. Effect of height of weir at water outlet on flooding

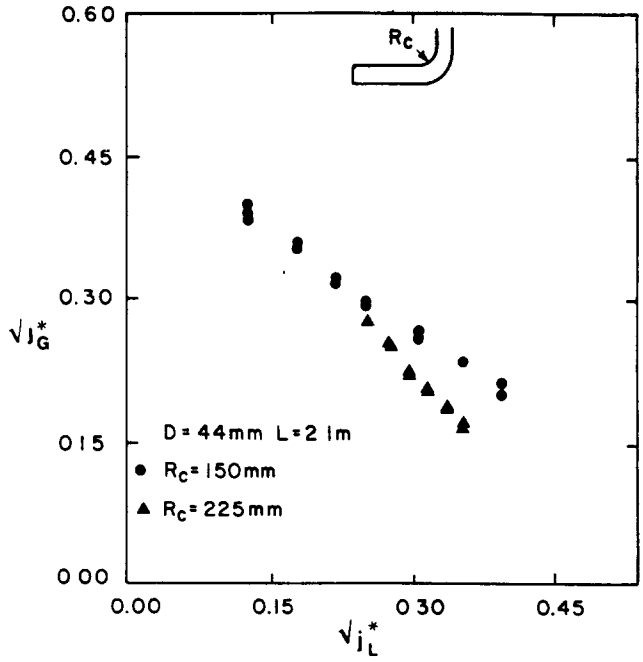

Figure 7. Effect of bend radius of curvature on flooding in a 44 mm I.D. pipe.

the hydraulic jump with the bend radius. Liquid coming into the bend is distributed as a film in the vertical section. As it goes through the bend, the liquid at the top drains to join the liquid stream at the bottom. The larger the bend radius the more complete the draining. This in turn may lead to a narrower, higher, hydraulic jump, and consequently a lower flooding rate.

Tube diameter effect. Figure 8 shows the effect of tube diameter on the onset of flooding. As is evident from the figure, there is an effect of tube diameter which is not accounted for by using the nondimensional groups j_G^* and j_L^*. Up to this point j_G^* and j_L^* have been convenient ways of displaying the data, because the parametric effect studies were done with tubes of the same diameter. The effect of diameter on the flooding behavior is discussed further in part II.

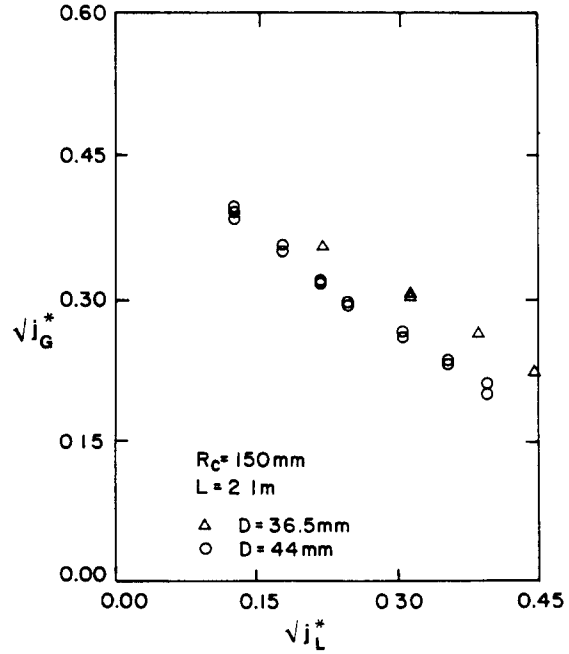

Figure 8. Effect of tube diameter on flooding in a 150 mm radius elbow

Entrance effects. Several other parameters can affect flooding behavior significantly For example, figure 9 shows the effect of exit geometry for the horizontal leg (at the air inlet/water outlet). Bell-shaped and square-edge air entrances were studied. All data discussed up to this point were taken from a square-edged exit geometry. It is seen from figure 9 that the use of a rounded exit geometry leads to a significant increase in the air flow rate needed to cause flooding. The reason for this effect is again unclear. In our experiments a free outfall existed at the exit of the horizontal pipe, implying that the liquid stream depth was close to the critical depth near the end of the tube. It is possible that with a bell-mouth exit geometry the curvature of the stream led to a reduction in the critical exit depth, and hence in the height of the hydraulic jump further upstream. This may have led to an increased air flow at flooding.

Effect of slight inclination of horizontal leg. Experiments were performed in which the lower leg of the elbow was slightly inclined, while the vertical leg was kept in the same position. A marked effect on the flooding behavior was seen, as shown in figure 10. For a slight upward inclination of 0.6° (i.e., a bend angle of 89.4°) the air flow rate needed to cause flooding is greatly reduced, whereas for an equal downward inclination (bend angle 90.6°) the contrary is seen. Such behavior is anticipated, since the liquid depth in the horizontal leg, and hence the height of the hydraulic jump where slugging occurred, were very sensitive to the inclination of the horizontal leg. In fact, for the case where the bend angle was greater than 90°, a hydraulic jump was difficult to discern for the case studied. The inclination effect is discussed in detail in part II.

3.3 Void fraction at onset of slugging

Photographic measurements were made of the height of the hydraulic jump at the onset of slugging, which corresponds to flooding inception in the present system. Results are plotted in figure 11 in terms of the local void fraction α_G at the crest of the hydraulic jump, and the nondimensional air superficial velocity j_G^*. The void fraction has been inferred from the height of the liquid level at the wall of the pipe. It was not possible to correct for possible variations in the level height across the width of the tube. In very rough terms it is seen that flooding occurs according to the equation

$$j_G^* = j_{Gc}^* \, \alpha_G^{3/2}, \qquad [1]$$

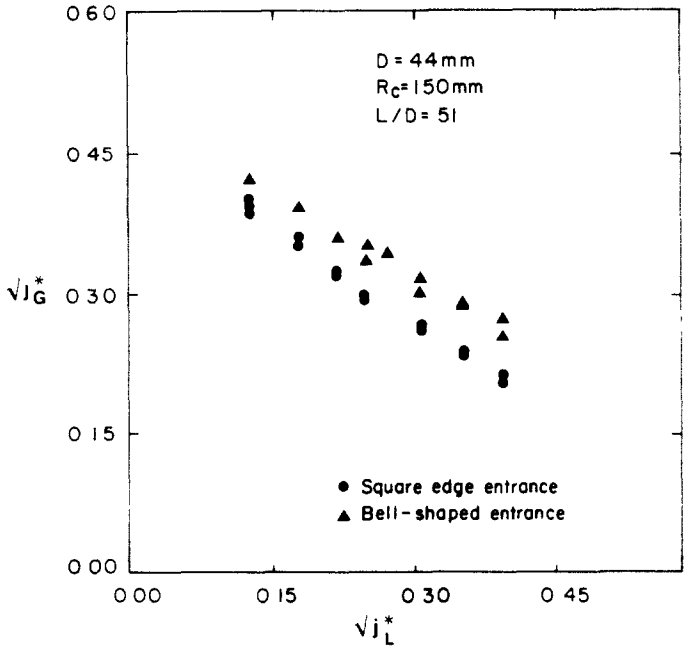

Figure 9 Effect of horizontal leg exit geometry on the onset of flooding

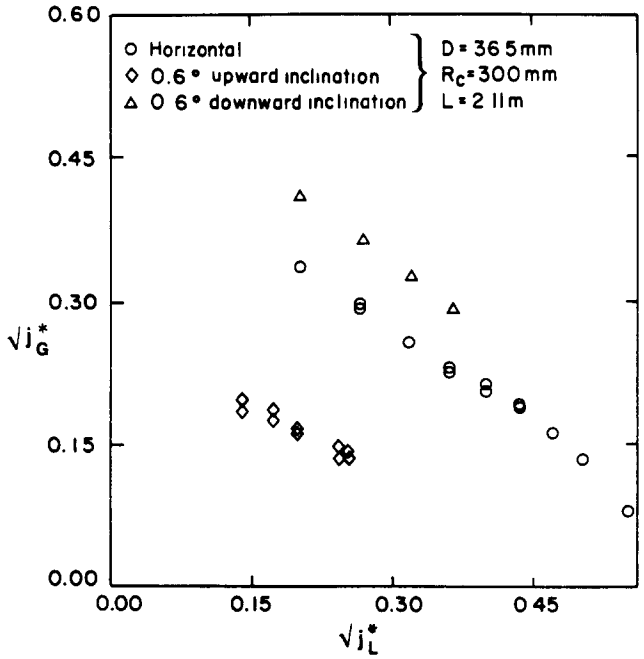

Figure 10. Effect of slight inclination of horizontal section on flooding behavior.

where j^*_{Gc} is a constant equal to 0.2. Wallis & Dobson (1973) measured air–water countercurrent flow limits in a horizontal rectangular channel. In their tests a constant liquid depth was maintained, and no hydraulic jump was present. Their data are also described by [1], but with $j^*_{Gc} = 0.5$ (see figure 11). The difference between the j^*_{Gc} values obtained by Wallis & Dobson and in our experiments is probably partly due to the difference in the duct cross-sectional shapes. Also, the presence of the hydraulic jump in our tests may have promoted the early inception of a local wave instability.

It is interesting to note that an equation of the form of [1] can be derived by performing a linear stability analysis on the governing equations for an inviscid stratified flow, as noted by Ardron (1980). This supports the idea that the wave instability is probably a classical Kelvin–Helmholtz instability.

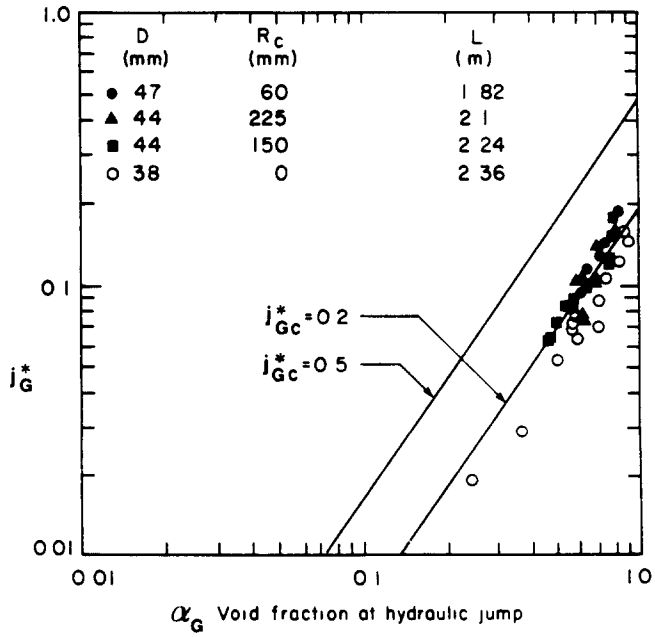

Figure 11. Minimum void fraction at hydraulic jump at onset of flooding.

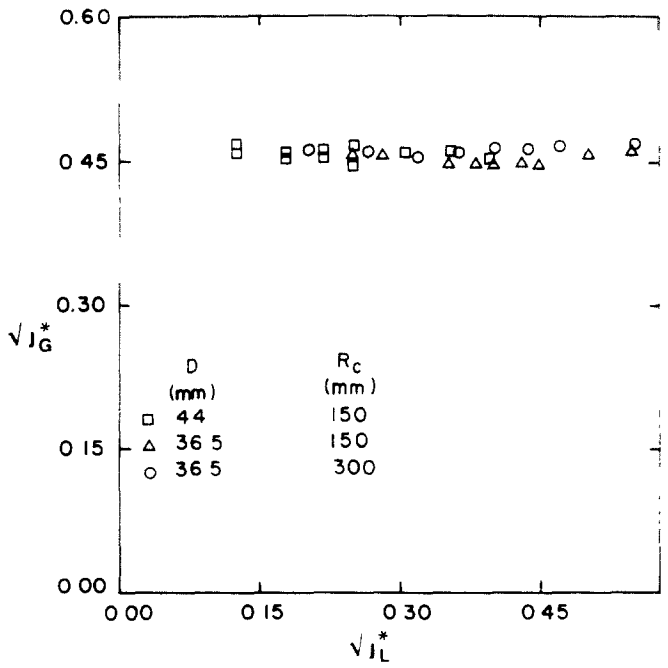

Figure 12 Air flow rate for total liquid carry-up

3.4 Complete carry-up limit

Figure 12 shows the air flow rate at which complete liquid carry-up, i.e., no liquid outflow at gas inlet, was just achieved, for a range of tube sizes. The liquid flow rate on the horizontal axis is the liquid supply rate to the sinter. The complete carry-up limit seems largely independent of tube diameter bend radius and the liquid supply rate, and is predicted reasonably well by

$$\sqrt{j_G^{*1/2}} = 0.45 . \qquad [2]$$

Beyond the complete carry-up limit liquid was still present in the horizontal section, but it did not now flow out of the gas inlet.

4 SUMMARY AND CONCLUSIONS

Experiments have been performed to measure flooding limits in air–water countercurrent flow in elbows consisting of a vertical upper limb and a lower limb which was horizontal or slightly inclined. Flooding was found to be caused by slugging at the hydraulic jump that formed in the lower leg of the elbow close to the bend.

The flooding limit was found to depend on the tube diameter, the length and inclination of the lower leg of the elbow, and the radius of curvature of the bend. Gas flow rates at flooding were well below those expected for flooding in vertical pipes, or for slugging in cocurrent flow in horizontal pipes.

A theoretical analysis leading to a flooding correlation, which incorporates the effects of the length and inclination of the lower leg of the elbow, is given in the second paper in this series (part II).

Acknowledgments—This work was partially supported by the National Science Foundation under Grant CPE 81-12667

REFERENCES

ARDRON, K. H. 1980 One-dimensional two-fluid equations for horizontal stratified two-phase flow. *Int. J. Multiphase Flow* **6**, 295–304.

KROWLEWSKI, S. M. 1980 Flooding limits in a simulated nuclear reactor hot-leg. Massachusetts Institute of Technology submission as part of requirement for a B.Sc.

PUSHKINA, O. L. & SOROKIN, Y. L. 1969 Breakdown of liquid film motion in verical tubes. *Heat Transfer — Soviet Research* **1**, 56–64.

RICHTER, H. J. 1981 Flooding in tubes and annuli. *Int. J. Multiphase Flow* **7**, 647–658.

RICHTER, H. J., WALLIS, G. B., CARTER, K. H. & MURPHY, S. L. 1978 De-entrainment and countercurrent air–water flow in a model PWR hot-leg. U.S. Nuclear Regulatory Commission Report NRC-0193-9.

SHEARER, C. J. & DAVIDSON, J. F. 1965 The investigation of a standing wave due to gas blowing upwards over a liquid film; its relation to flooding in wetted-wall columns. *J. Fluid Mech.* **22**, 321–335.

TAITEL, Y. & DUKLER, A. E. 1976 A model for predicting flow regime transitions in horizontal and near horizontal gas–liquid flow. *AIChE J.* **22**, 47–55.

TIEN, C. L., CHUNG, K. S. & LUI, C. P. 1979 Flooding in two-phase countercurrent flows. Electric Power Research Institute Report EPRI-NP-1283 72.

WALLIS, G. B. 1969 *One-dimensional Two-phase Flow,* Chap. 6. McGraw-Hill, New York.

WALLIS, G. B. & DOBSON, J. E. 1973 The onset of slugging in horizontal stratified air–water flow. *Int. J. Multiphase Flow* **1**, 173–193.